Available online at www.sciencedirect.com
ScienceDirect
Trans. Nonferrous Met. Soc. China 24(2014) 2187−2195
Transactions of Nonferrous Metals Society of China
www.tnmsc.cn

Mechanical properties of 7475 aluminum alloy sheets with fine subgrain structure by warm rolling

Hiroki TANAKA, Tadashi MINODA

Research and Development Center, Sumitomo Light Metal Ind. Ltd., 3-1-12, Chitose, Minato-ku, Nagoya 455-8670, Japan

Received 17 October 2013; accepted 3 December 2013

Abstract: The effect of transition elements on grain refinement of 7475 aluminum alloy sheets produced by warm rolling was investigated. The alloy which contains zirconium instead of chromium showed ultra fine structures with stable subgrains after warm rolling at 350 °C, followed by solution heat treatment at 480 °C. The average subgrain diameter was approximately 3 μm. It became clear that zirconium in solution has the effect of stabilizing subgrains due to precipitation of fine Al_3Zr compounds during warm rolling. On the other hand, chromium-bearing compounds precipitate before warm rolling and they grow up to relatively large size during warm rolling. The warm rolled sheets with fine subgrains have unique properties compared with conventional 7475 aluminum alloy sheets produced by cold rolling. The warm rolled sheets solution heat treated had subgrain structures through the thickness with a high proportion of low-angle boundary less than 15°. The strength of the warm rolled sheets in T6 condition was about 10% higher than that of conventional 7475 aluminum alloy sheets. As the most remarkable point in the warm rolled sheets, the high Lankford (r) value of 3.5 was measured in the orientation of 45° to rolling direction, with the average r-value of 2.2. The high r-value would be derived from well developed β-fiber textures, especially with the strong $\{011\}\langle 211\rangle$ brass component. The warm rolled sheets also had high resistance to SCC. From Kikuchi lines analysis and TEM images, it was found that PFZs were hardly formed along the low-angle boundaries of the warm rolled sheets in T6 condition. This would be a factor to lead to the improvement of resistance to SCC because of reducing the difference in electrochemical property between the grain boundary area and the grain interior.

Key words: warm rolling; aluminum−zinc−magnesium−copper; grain refinement; stress corrosion cracking

1 Introduction

In order to use wrought aluminum alloys for structural components, it is important to improve their mechanical properties in resistance to corrosion and formability as well as strength for high reliability, good design and weight saving. It is well known in low-carbon steels that yield stress has a relation with grain size [1,2], and the relation can be applied to aluminum alloy sheets. The grain refinement of aluminum alloy sheets is one useful method to achieve high strength. On the other hand, it was reported that the grain refinement of 7075 aluminum alloy sheets has a disadvantage on resistance to stress corrosion cracking (SCC) [3]. It would be difficult to establish a process that can achieve the improvement of all properties mentioned above at the same time. Therefore, in practical use, some of the mechanical properties should be improved moderately according to circumstances where materials are used. In the previous study [4], it was revealed that the control of the second phase distributions and solution elements leads to fine structure about 7 μm in average grain diameter in 7475 aluminum alloy sheets by cold rolling after solution heat treatment. It was also revealed in the prior study [5] that control of roll temperature is important to form thermal stabilized structure of 7000 series aluminum alloy sheets. In the study, a new type of roll embedded cylindrical heater was used to prevent reduction of sample temperature in the rolling process. Hereafter, this type of rolling is called controlled warm rolling.

The objective of the present work is to form finer structure in 7475 aluminum alloys by the controlled warm rolling which can control subgrain stability and to clarify mechanical properties of the warm rolled sheets

Corresponding author: Hiroki TANAKA; E-mail: tanaka-hiroki@uacj.co.jp
DOI: 10.1016/S1003-6326(14)63331-8

compared with conventional 7475 aluminum alloy sheets produced by cold rolling.

2 Experimental

Table 1 shows the chemical compositions of Al−Zn−Mg−Cu alloys used in this study. The mark M means an 7475 aluminum alloy containing zirconium instead of chromium. The mark S means a conventional 7475 aluminum alloy. The both alloys were cast into slabs as shown in Table 2 by a standard semi-continuous direct chill technique. The slabs were homogenized at 470 °C for 10 h followed by pre-heating at 350 °C for 10 h before forging at 350 °C. In the forging stage, a sample was compressed from 100 mm to 30 mm in thickness. The forged samples were machined with dimensions of 30 mm (height), 200 mm (width) and 100 mm (length). These blocks were rolled at 350 °C with re-heating at 350 °C for 1800 s after every two passes up to 4 mm in thickness followed by every pass up to 1 mm in thickness. 27 rolling passes (one pass reduction; 2 mm per pass up to 10 mm in thickness, 1 mm per pass up to 9 mm thickness and 0.5 mm per pass up to 1 mm in thickness) were carried out in total and the sheets were finally prepared with dimensions of 1 mm (thickness) and 200 mm (width).

Table 1 Chemical composition of specimens (mass fraction, %)

Alloy	Si	Fe	Cu	Mn	Mg
M	0.02	0.03	1.64	<0.01	2.40
S	0.04	0.03	1.51	<0.01	2.26
Alloy	**Cr**	**Zn**	**Ti**	**Zr**	**Al**
M	<0.01	5.55	0.03	0.17	Bal.
S	0.21	5.38	0.04	<0.01	Bal.

Table 2 Experimental procedure on warm rolling

Stage	Condition
Casting	Semicontinuous direct chill techniques into slab
Homogenization	470 °C, 10 h
Pre-heating	350 °C, 10 h
Forging	350 °C, 100 mm→30 mm
Machining	30 mm×200 mm×100 mm
Warm rolling	350 °C, re-heating/pass, 27 passes (30 mm→1 mm)
Annealing	350 °C, 30 min
Solution heat treatment	480 °C, 5 min, WQ
Artificial aging	120 °C, 24 h

The surface temperatures of the rolls were controlled at approximately 100 °C by cylindrical heaters. The roll was 160 mm in diameter and rotated 120 revolutions per minute. Commercial machine oil was used in the warm rolling process.

Regarding alloy S, other sample sheets were also produced by conventional process in order to compare mechanical properties with the warm rolled sheets. Hot rolled plates of alloy S were produced under conventional conditions. The plates were heated as the intermediate annealing at 480 °C for 2 h followed by furnace cooling, then rolled to 1 mm in thickness at an ambient temperature. Solution heat treatment was carried out at 480 °C for 5 min followed by quenching into water immediately (T4 condition). After the quenching, artificial aging was carried out at 120 °C for 24 h (T6 condition).

Microstructure was observed using an optical microscope and a transmission electron microscope (TEM). Misorientation angles between grains were measured using electron backscattered diffraction (EBSD) equipment with a scanning electron microscope (SEM). X-ray diffraction method was used to describe incomplete pole figures, and orientation distribution functions (ODFs) were calculated from three incomplete pole figures of {111}, {110} and {100} by the harmonic method [6]. The ODFs were displayed using Bunge's system [5]. The mechanical properties of the samples in T6 condition were investigated. Tensile test specimens were got from the orientations of 0°, 45° and 90° to the rolling direction. The specimens for limiting draw ratio (LDR) measurement were annealed at 360 °C for 2 h followed by furnace cooling [7] (O temper) to ensure deep drawing property. LDR measurement was carried out with a punch of 33 mm in diameter under hold-down force of 3.9 kN. The test method of resistance to stress corrosion cracking (SCC) in T6 condition was based on Japanese industrial standard, JIS H8711. The specimens for this test were prepared from the orientation of 90° to the rolling direction, and were immersed in a solution containing 3.5% sodium chloride for 10 min followed by drying at 25 °C for 50 min with addition of stress controlled at 85% of yield strength. The above cycle was repeated until the specimens failed. The resistance to SCC was estimated by a time to failure of the specimens. Exfoliation corrosion susceptibility was examined with specimens in T6 condition by immersion for 9 h in a solution containing 4 mol/L sodium chloride, 0.5 mol/L potassium nitrate, and 0.1 mol/L nitric acid at 25 °C. The susceptibility to exfoliation was determined by visual examination according to the standard photographs in

ASTM G34. Specimens of fatigue test were got parallel to the rolling direction and machined with dimensions shown in Fig. 1. In this work, the axial loading fatigue test was conducted at room temperature with the stress ratio of 0.1 and the cyclic frequency of 30 Hz.

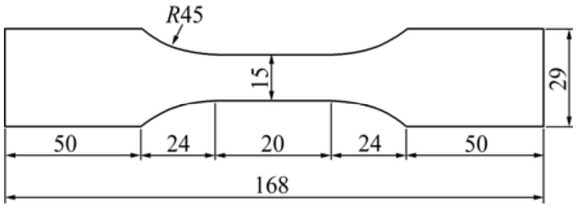

Fig. 1 Shape and dimensions of fatigue specimen (unit: mm)

3 Results

3.1 Microstructure in T4 condition

Figure 2 shows optical microstructures of warm rolled sheets after solution heat treatment. The structure of alloy M shows finer grains than that of alloy S. In alloy M, fine precipitates are confirmed in TEM observation (Fig. 3). These precipitates are identified as Al_3Zr of $L1_2$ structure tending to be coherent with the matrix. This is a reason to inhibit formation of large grains. In alloy S, larger precipitates were confirmed as $Al_{18}Cr_2Mg_3$ phase. These precipitates tend to be incoherent with the matrix, and they have less effect on inhibiting recrystallization.

In the following sections, properties of the warm rolled sheets of alloy M are compared with those of the cold rolled sheets of alloy S.

Figure 4 shows microstructures of both the warm rolled (alloy M) and cold rolled sheets (alloy S) in T4 condition. In optical micrographs, it is found that the cold rolled sheet (CR) consists of equiaxed grains about 20 μm in diameter, whereas the warm rolled sheet (WR) maintains fibrous structure as mentioned above. In TEM, it is revealed that the warm rolled sheet consists of fine grains whose average diameter is approximately 3 μm. As mentioned above, fine particles are judged as Al_3Zr in alloy M (warm rolled sheet) and $Al_{18}Cr_2Mg_3$ in alloy S (cold rolled sheet).

3.2 Distribution of misorientation angle in T4 condition

Figure 5 shows misorientation angle histograms taken from SEM-EBSD measurements. The measured area in this work was 100 μm×200 μm. The warm rolled sheets have a high proportion of low-angle boundary less than 15°, whereas the cold rolled sheet has a high proportion of high-angle boundary. According to this measurement, it is clear that the warm rolled sheet consists of subgrain structure.

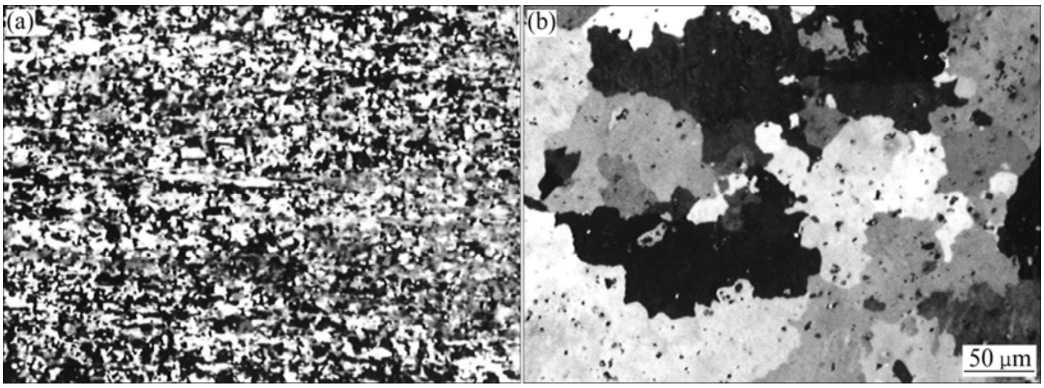

Fig. 2 Optical microstructure after solution heat treatment: (a) Alloy M; (b) Alloy S

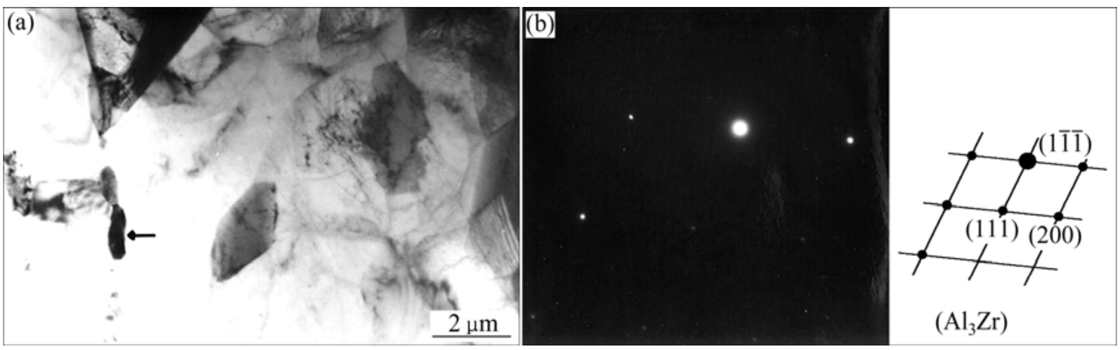

Fig. 3 TEM image (a) and SAD pattern (b) of alloy M after forging at 350 °C

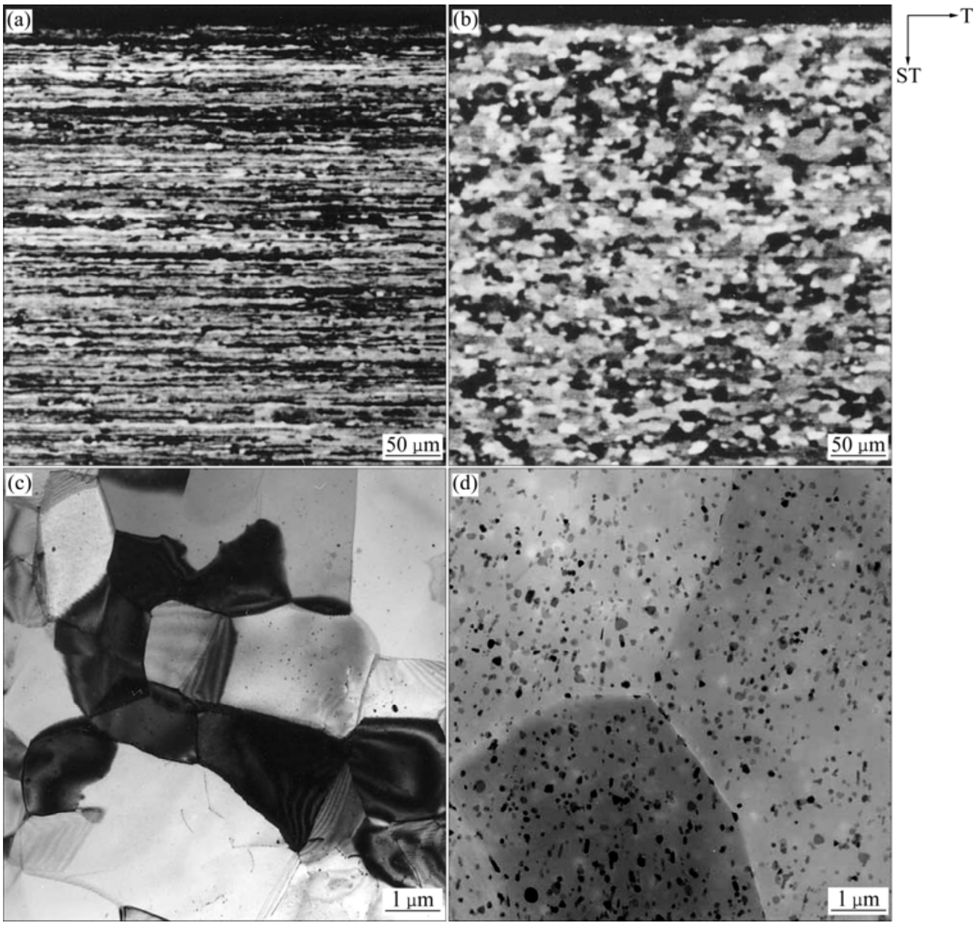

Fig. 4 Optical (a, b) and TEM (c, d) micrographs of alloys in T4 condition: (a, c) Warm rolled sheet, alloy M; (b, d) Cold rolled sheet, alloy S

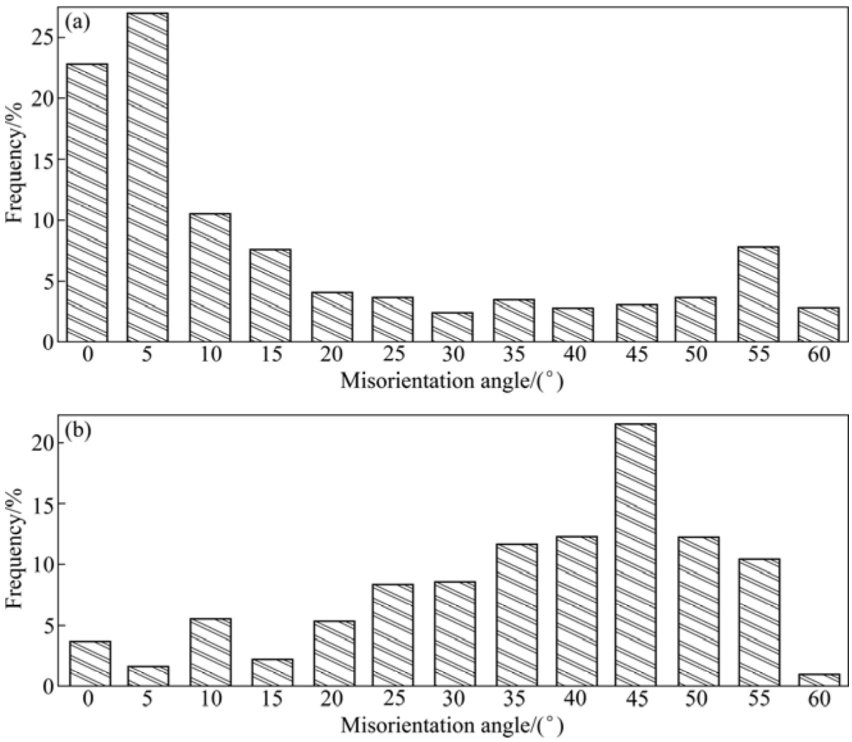

Fig. 5 Misorientation angle histograms of warm rolled sheet (a) and cold rolled sheet (b) in T4 condition

3.3 Tensile properties and LDR measurements

Table 3 summarizes tensile test results in T6 condition. The tensile strength of the warm rolled sheet is about 10% higher in orientations of 0° and 90° to rolling direction than that of the cold rolled sheet, and the tensile strength in 45° direction is almost in the same level for the both sheets. The warm rolled sheet has an anisotropy on ductility, whereas the cold rolled sheet tends to be isotropic on it as well as tensile and yield strengths.

Table 3 Mechanical properties of warm rolled sheet and cold rolled sheet in T6 condition

Condition	Angle to RD/(°)	Tensile strength/ MPa	Yield strength/ MPa	Elongation/ %
Alloy M in WR-T6	0	592	496	13
	45	522	461	19
	90	601	455	13
Alloy S in CR-T6	0	522	461	16
	45	521	457	17
	90	526	468	16

Figure 6 shows the plastic strain ratio of width to thickness (Lankford value: *r*-value) measured at 10% elongation. It is remarkable point that the warm rolled sheet has a quite high value over 3.5 in the orientation of 45° to the rolling direction. The warm rolled sheet also shows anisotropy on *r*-value. The average *r*-value of the warm rolled sheet is 2.2, meanwhile, that of the cold rolled sheet is 0.6. LDR measurements show that the warm rolled sheet tends to have a higher value (2.06) than the cold rolled sheet (2.00), and it is found that the LDR values have correlation with the average *r*-values shown in Fig. 6.

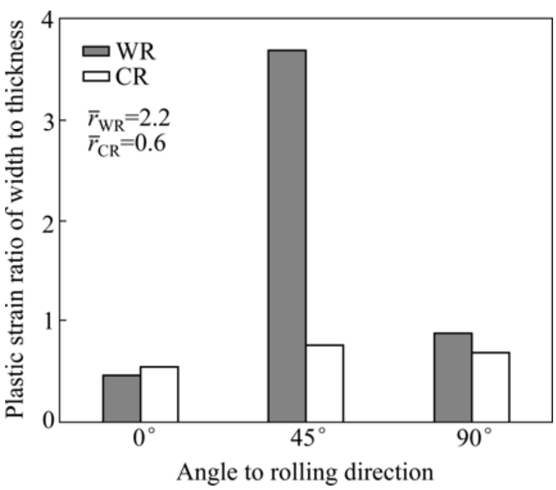

Fig. 6 Plastic strain ratio of width to thickness in T6 condition (WR: Warm rolled sheet; CR: Cold rolled sheet; $\bar{r}$: Average *r*-value)

3.4 Corrosion resistance

Figure 7 shows the life of SCC in T6 condition. The warm rolled sheets have better resistance to SCC than the cold rolled sheets. Figure 8 shows the appearance and photomicrographs of the L-ST section after the immersion test. The both sheets have the same classification and are estimated to be EA.

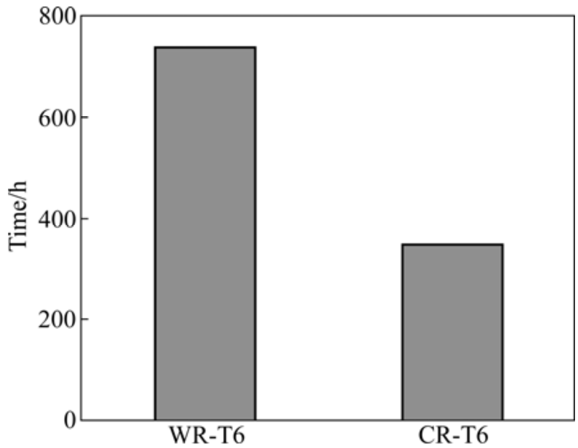

Fig. 7 Life of SCC in T6 condition (WR: Warm rolled sheet; CR: Cold rolled sheet)

3.5 Fatigue strength

Figure 9 gives stress−number curves of the samples in T6 condition. The fatigue strength of the warm rolled sheets is about 10% higher than that of the cold rolled sheets. It is well known that fatigue strength increases with increasing tensile strength [8]. Furthermore, the effect of the fibrous structure in the warm rolled sheets on the fatigue strength should be examined in future.

4 Discussion

One of remarkable properties on the warm rolled sheets is high *r*-value shown in Fig. 6. According to the previous work [9] based on Taylor theory [10], it was predicted that the *r*-value of 45° orientation would be increased by a {011}⟨211⟩ brass component. Figure 10 shows the ODFs in the surface layer and at center layer of the samples used in this work. The {011}⟨211⟩ brass component is formed strongly through the thickness of the warm rolled sheet. Another orientation near a {123}⟨634⟩ S component was perceived but its orientation density was lower than that of the brass component. It is well known that β-fiber orientations involve brass, S and C components. However, a {112}⟨111⟩ C component was not perceived through the

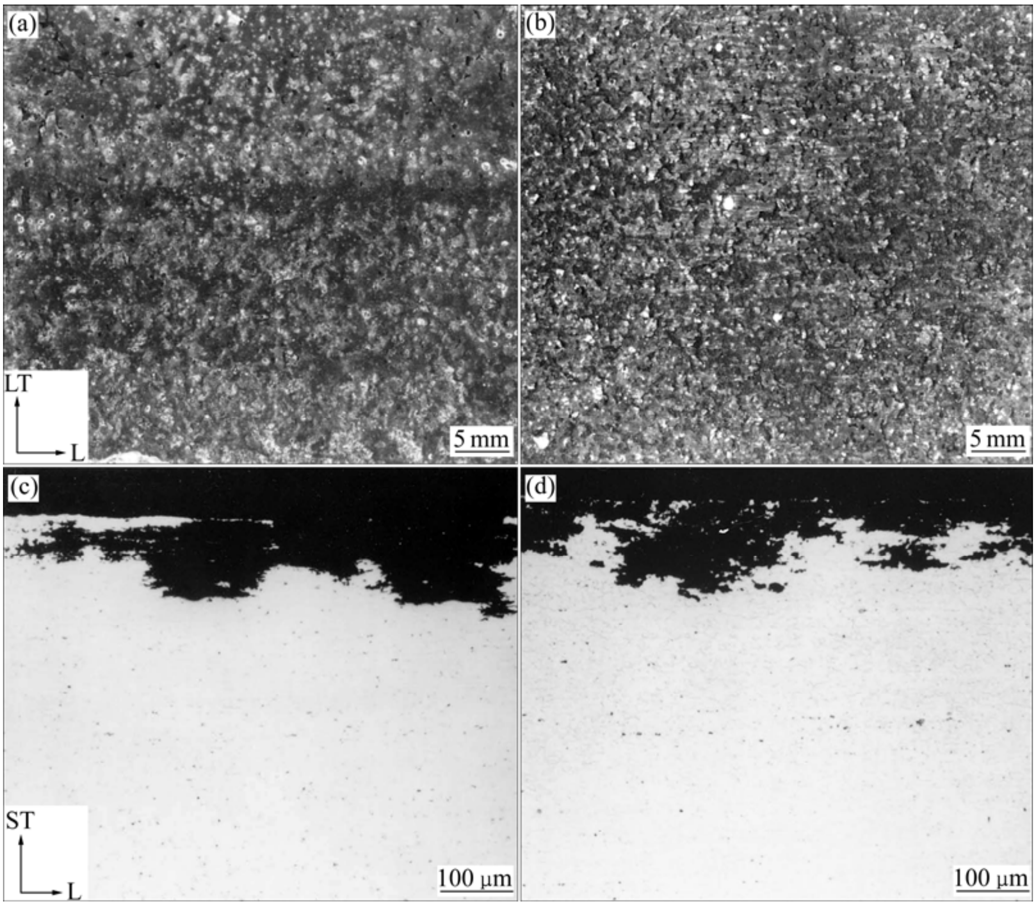

Fig. 8 Appearance and photomicrographs showing cross sections of warm rolled sheet (WR) (a, c) and cold rolled sheet (CR) (b, d) exposed to test solution for 9 h

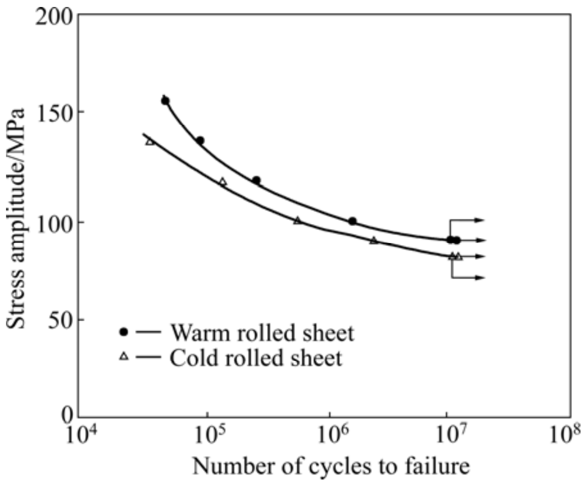

Fig. 9 Stress−number cycle curves for specimens in T6 condition

thickness of the warm rolled sheet. According to the above texture analysis, the high r-value of the orientation of 45° in the warm rolled sheet will be derived from the high orientation density of the brass component. The present results are in agreement with the previous work [8] mentioned above. Regarding to the cold rolled sheets, as shown in Fig. 10, ND- and RD-rotated cube components as well as a $\{011\}\langle 100\rangle$ Goss component are perceived. Their orientation densities are much lower than the brass component in the warm rolled sheets. Besides of these quite well defined recrystallization texture components, the ODFs comprise the random component. Accordingly, the very weak recrystallization textures with the random component will lead to isotropic tensile properties of the cold rolled sheets. The cold rolled sheets consisted of β-fiber components in as-rolled condition, but the orientation density of the brass component before solution heat treatment was much lower than that of the warm rolled sheets [11]. It would be thought that the strong brass component in the warm rolled sheets is due to the formation of fine subgrain structure that is quite stable thermally.

In the present work, specimens in O-temper were used for LDR measurements. This O-temper treatment was carried out at 360 °C after solution heat treatment at 480 °C, so that it was confirmed that the textures of specimens did not change by the O-temper treatment. Based on this confirmation, it would be found that the average r-values have correlation with the LDR

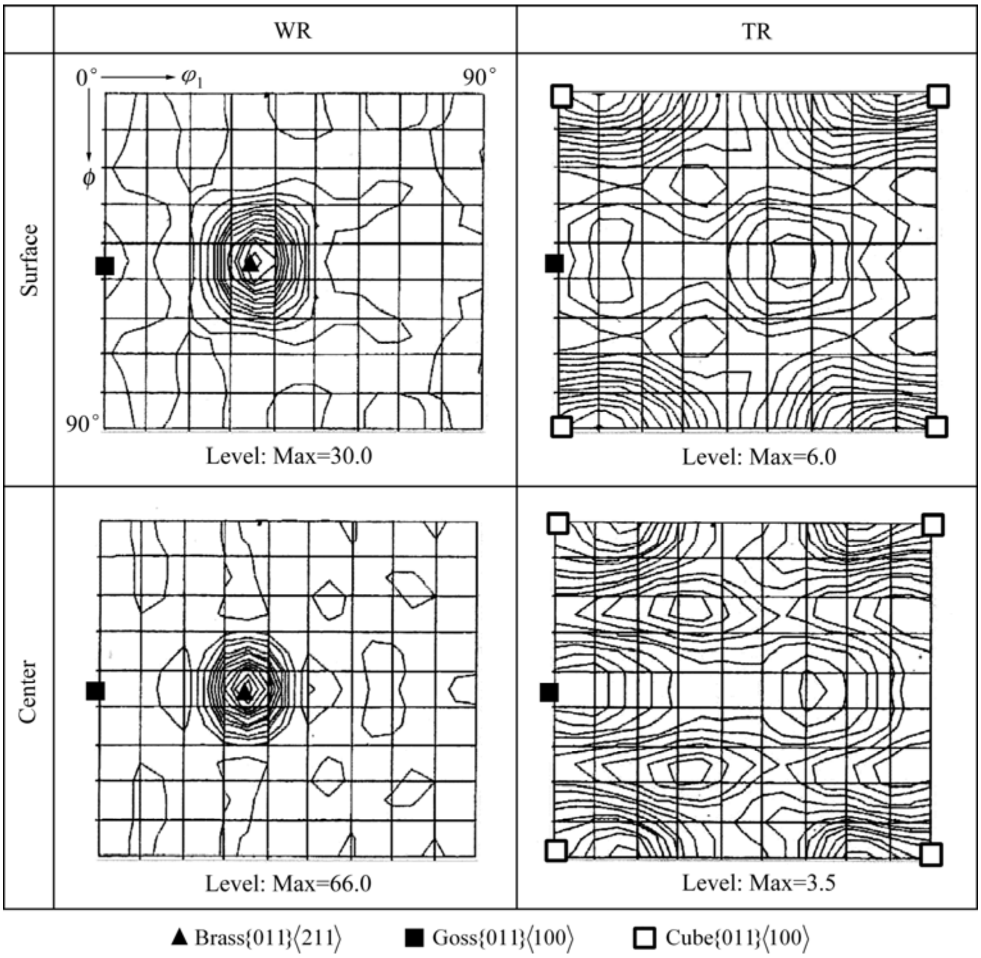

Fig. 10 ODFs of warm rolled sheet (WR) and cold rolled sheet (CR) in T4 condition (φ_2=0°)

values. It would be another subject that precipitation condition may affect drawing properties, but this consideration is beyond the scope of the present work.

In the previous work [12], influence of alloying elements in 7075 aluminum alloys was investigated. It was found in the work that addition of zirconium brought about reduction of SCC life in T6 condition. The reason why the warm rolled sheets containing zirconium have good resistance to SCC may be derived from their microstructure. In the previous study on 6061 aluminum alloy extrusions [13], it was suggested that the formation of a precipitate free zone (PFZ) is restrained at a low-angle boundary, which leads to high resistance to intergranular corrosion. Figure 11 shows TEM images of the samples in T6 condition and Kikuchi patterns derived from two grains facing each other across a grain boundary. From Kikuchi pattern analysis, it was confirmed that a low-angle boundary is observed in the warm rolled sheet and a high-angle boundary is observed in the cold rolled sheet. It is clearly found that a PFZ is restrained at the low angle boundary, whereas a PFZ is formed distinctly at the high-angle boundary. Other grain boundary areas of the both sheets showed the same characteristic on the PFZ formation. In the case of narrow PFZ formation, the difference of electrochemical property between the grain boundary area and the grain interior tends to reduce, which would prevent a partial anodic reaction and lead to the improvement of resistance to SCC [14,15].

5 Conclusions

1) The warm rolled sheets of 7475 aluminum alloy containing zirconium instead of chromium show fine subgrain structures after solution heat treatment. The warm rolled sheets also show the high r-value of 3.5 in the orientation of 45° to rolling direction due to well developed β-fiber components, especially with the strong{011}⟨211⟩ brass component after solution heat treatment.

2) The average r-value of the warm rolled sheets is higher than that of the cold rolled sheets, so that the warm rolled sheets have better deep drawing properties in O-temper.

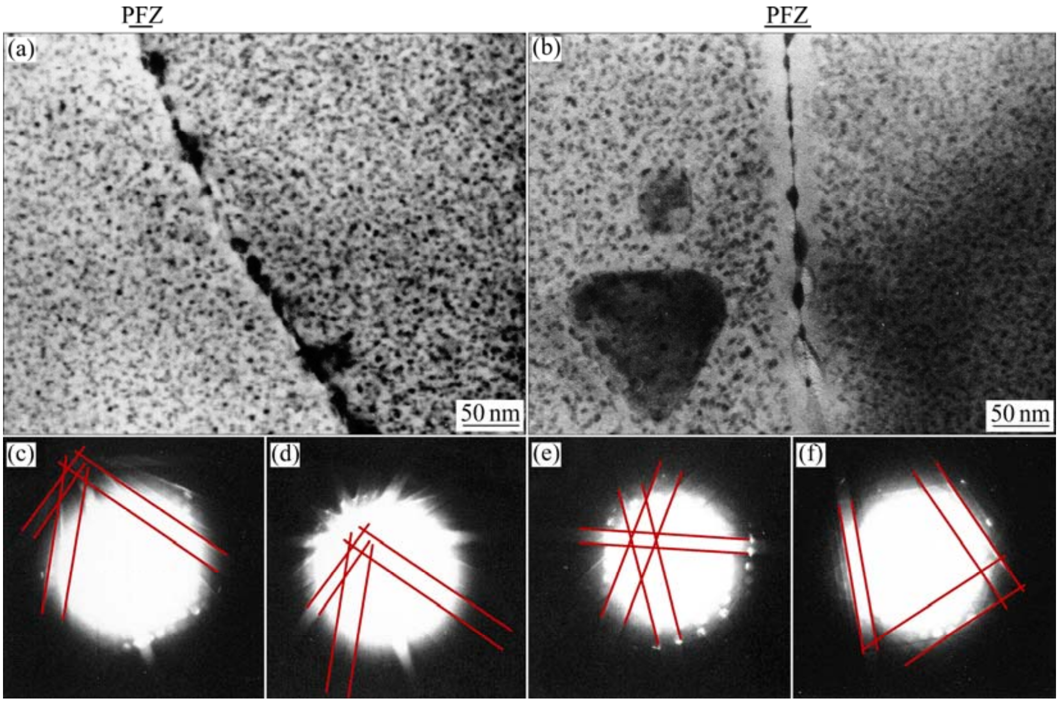

Fig. 11 TEM images (a, b) and Kikuchi patterns (c−f) in T6 condition: (a, c, d) Warm rolled sheet; (b, e, f) Cold rolled sheet; (c, d) WR (Misorientation angle 5°); (e, f) CR (Misorientation angle 41°)

3) PFZ is hardly formed along the low angle boundaries of the warm rolled sheets in T6 condition, which would lead to the improvement of resistance to SCC because of the uniformity of electrochemical property between the grain boundary area and the grain interior.

4) The fatigue strength of the warm rolled sheets in the orientation of 0° to rolling direction is about 10% higher than that of the cold rolled sheets.

Acknowledgment

This work was supported in part by a research fund of the Super Aluminum Project provided by the Japan Research and Development Center for Metals (JRCM) in the New Energy and Industrial Technology Development Organization (NEDO). The authors thank JRCM and NEDO for the permission of publication of this report. The authors also acknowledge Professor Z. HORITA, Kyushu University in Japan, for the measurements of the grain boundary misorientations by Kikuchi lines of TEM images.

References

[1] DIETER G E. Mechanical metallurgy [M]. New York: McGraw-Hill Int., 1986: 189.
[2] ABSON D J, JONAS J J. The Hall-Petch relation and high-temperature subgrains [J]. Metal Science Journal, 1970, 4(1): 24−28.
[3] The Society of Japan Aerospace Companies. Investigation for the promotion of aero parts and materials industries No.807 [R]. 1994.
[4] YOSHIDA H. Role of second phase particles and solute atoms in the grain refinement of a 7475 alloy sheet [J]. Journal of Japan Institute of Light Metals, 1991, 41: 331−337.
[5] TANAKA H, MINODA T, ESAKI H, SHIBUE K, YOSHIDA H. [C]//Proceedings of 8th International Conference ICAA8. Cambridge, UK, 2002: 499.
[6] BUNGE H J. Texture analysis in materials science [M]. London: Butterworths, 1982.
[7] HIRANO S, YOSHIDA H. Effect of manganese on n value of Al−Mg−Si alloys [J]. Sumitomo Light Metal Technical Reports, 1997, 38: 1−6.
[8] TAKEUCHI K. [J]. Journal of Light Metal Welding and Construction, 1966, 4: 184.
[9] INOUE H, INAKAZU N. Measurement and analysis of crystallographic texture [J]. Journal of Japan Institute of Light Metals, 1994, 47(4):246−257. (in Japanese)
[10] TAYLOR G I. Plastic strain in metals [J]. J Inst Metals, 1938, 62: 307−324.
[11] TANAKA H, MINODA T, ESAKI H, SHIBUE K, YOSHIDA H. [J]. Journal of Japan Institute of Light Metals, 2002, 52: 231−235.
[12] The Society of Japan Aerospace Companies. Investigation for the promotion of aero parts and materials industries No.904 [R]. 1995.
[13] MINODA T, YOSHIDA H. Effect of grain boundary characteristics on intergranular corrosion resistance of 6061 aluminum alloy extrusion [J]. Metallurgical and Material Transactions A, 2002, 33: 2891−2898.
[14] POUGH E N, JONES W R D. The mechanism of stress-corrosion in a high purity aluminum−zinc−magnesium alloy[J]. Metallurgia, 1961, 63: 3.
[15] MURAKAMI Y. [J]. Journal of Japan Institute of Light Metals, 1981, 31: 74.

温轧细化亚晶 7475 铝合金板材的力学性能

Hiroki TANAKA, Tadashi MINODA

Research and Development Center, Sumitomo Light Metal Ind. Ltd., 3-1-12, Chitose, Minato-ku,
Nagoya 455-8670, Japan

摘　要：研究了温轧下过渡元素对 7475 铝合金板材晶粒细化的影响。经 350 °C 温轧、480 °C 固溶热处理后，用 Zr 代替 Cr 的 7475 铝合金具有稳定亚晶超细组织；平均亚晶直径接近 3 μm。结果表明，溶液中的 Zr 能稳定亚晶是因为温轧中析出了细小的 Al_3Zr 粒子；另一方面，含 Cr 粒子化合物在温轧之前析出，并且在温轧过程中会变粗大。与传统冷轧 7475 铝合金板材相比，温轧细化亚晶板材具有独特的性能。固溶处理后的温轧板材，在厚度截面的亚晶组织具有高比例小于 15°的小角度晶界；温轧 T6 态合金板材的强度高于传统 7475 铝合金板材强度 10%。温轧铝合金板材最显著的特点是，在与轧制方向呈 45°时高 Lankford(r)值为 3.5，而其平均 Lankford(r)值为 2.2。高 Lankford(r)值有利于组织演变为 β-fiber 织构，特别是强{011}⟨211⟩黄铜部分。同时，温轧板材也具有高的抗应力腐蚀开裂性能(SCC)。根据 Kikuchi 线和透射电镜分析，温轧 T6 板材形成的小角度晶界导致无沉淀析出带(PFZs)难以形成，这是导致抗应力腐蚀开裂性能提高的重要因素，其原因是晶界和晶内的电化学性能存在差异。

关键词：温轧；Al−Zn−Mg−Cu；晶粒细化；应力腐蚀开裂

(Edited by Hua YANG)